Results in Physics 7 (2017) 1818–1823

Contents lists available at ScienceDirect

Results in Physics

journal homepage: www.journals.elsevier.com/results-in-physics

Ether gas-sensor based on Au nanoparticles-decorated ZnO microstructures

Roberto López [a,*], Enrique Vigueras-Santiago [b], Alfredo Rafael Vilchis-Nestor [c], Victor Hugo Castrejón-Sánchez [d], Marco A. Camacho-López [b], Nayely Torres-Gómez [e]

[a] División de Ingeniería Mecatrónica, Tecnológico de Estudios Superiores de Jocotitlán (TESJo), Carretera Toluca-Atlacomulco km 44.8, Ejido de San Juan y San Agustin, Jocotitlán, Edo. México, Mexico
[b] Laboratorio de Investigación y Desarrollo de Materiales Avanzados (LIDMA), Facultad de Química, Universidad Autónoma del Estado de México, Paseo Colón esquina Paseo Tollocan, Toluca, Estado de México, Mexico
[c] Centro Conjunto de Investigación en Química Sustentable UAEM – UNAM, Carretera Toluca-Atlacomulco, km 14.5, Unidad El Rosedal, C.P. 50200, Toluca, Estado de México, Mexico
[d] Tecnológico de Estudios Superiores de Jocotitlán (TESJo), Carretera Toluca-Atlacomulco km 44.8, Ejido de San Juan y San Agustin, Jocotitlán, Edo. México, Mexico
[e] Estudiante del programa de Doctorado en Ciencia de Materiales de la, Universidad Autónoma del Estado de México, Paseo Colón esq. Paseo Tollocan, Toluca, Mexico

ARTICLE INFO

Article history:
Received 4 March 2017
Received in revised form 16 May 2017
Accepted 21 May 2017
Available online 22 May 2017

Keywords:
ZnO microstructures
Au nanoparticles
Ether
Gas sensor

ABSTRACT

An ether gas-sensor was fabricated based on gold nanoparticles (Au-NPs) decorated zinc oxide microstructures (ZnO-MS). Scanning electron microscope (SEM) and high-resolution transmission electron microscope (HRTEM) measurements were performed to study morphological and structural properties, respectively, of the ZnO-MS. The gas sensing response was evaluated in a relatively low temperature regime, which ranged between 150 and 250 °C. Compared with a sensor fabricated from pure ZnO-MS, the sensor based on Au-NPs decorated ZnO-MS showed much better ether gas response at the highest working temperature. In fact, pure ZnO-MS based sensor only showed a weak sensitivity of about 25%. The improvement of the ether gas response for sensor fabricated with Au-NPs decorated ZnO-MS was attributed to the catalytic activity of the Au-NPs.

Introduction

Diethyl ether, more commonly known as ether, highly volatile liquid of characteristic odor, has been widely used in several industrial and medical applications. Among them, it is frequently employed as a solvent for a wide range of substances, including fats, oils and waxes [1–4]. Many years back, ether was used as anesthetic agent for humans. However, it is extremely pungent, highly flammable, and explosive. Continual exposure to ether may lead to nervous systems effects such as dizziness, drowsiness, loss of consciousness or even death [5,6]. Thus, the hazardous characteristics of ether make monitoring it in air necessary. Most works reporting gas sensors of ether used chemiluminescence for detection of it [7–9], although some metal oxides such as titanium dioxide and zinc oxide (ZnO) could be an alternative for fabrication of ether gas sensors due to they have shown interesting characteristics in sensing of volatile organic compounds such as acetone and ethanol. ZnO is an n-type semiconductor with an energy gap of 3.37 eV at room temperature. It has been used for several applications due to its electrical, catalytic, and photoelectronic properties [10–13]. It has been employed as a chemical gas sensor due to its high mobility of electrons and excellent chemical and thermal stability under operation conditions of the sensor [14–19]. The gas sensing mechanism in ZnO is explained on the basis of electron interchange between adsorbed oxygen ions and the surface of ZnO.

As most metal oxides, operating temperature for ZnO gas sensors should be kept at least at a minimum temperature of 300 °C or even higher temperatures since O^- ion is believed to be dominant at such working temperatures [20]. One method for improving the ZnO gas response for some gases is through surface modification or doping. For example, several metals have been used as additives to ZnO in order to increase sensitivity of the sensor [21,22]. Among them, doping or decoration of ZnO with gold nanoparticles (Au-NPs) have shown to be an efficient way to improve gas response to several gases such as CO, NO_2, ethanol, and acetone [23–25]. Recently, some attempts have been made to detect other organic vapors such as ether with ZnO [16]. However, gas response from those sensors is weak compared to that obtained from other volatile organic compounds such as ethanol and acetone. In the current work, it is shown that sensors fabricated with Au-NPs deposited on the surface of ZnO microstructures

* Corresponding author.
E-mail address: lorr810813@gmail.com (R. López).

http://dx.doi.org/10.1016/j.rinp.2017.05.019
2211-3797/

(ZnO-MS), exhibit an efficient gas response to ether when are compared with those fabricated with pure ZnO-MS. Such sensors were characterized at a relatively low working temperature of 250 °C.

Materials and methods

The sensor for ether gas detection was fabricated using Au-NPs decorated ZnO-MS. Synthesis of ZnO-MS is described as follows: a solution of 2 mM of Zn $(NO_3)2{\cdot}6H_2O$ in deionized water was maintained under magnetic stirring for 10 min. After that, 64% hydrazine was added to the solution, which was then transferred to an autoclave and placed at 180 °C in a muffle furnace for four hours. The obtained precipitate was filtered and washed several times with deionized water, and dried at 70 °C for 24 h. For biosynthesis of Au-NPs; 10 ml of a 1 mM aqueous solution of $HAuCl_4.XH_2O$ was added drop wise to 3 ml of *Camellia sinensis* extract (Table 1 shows details about formula, purity and manufacturer of each reagent used for synthesis of ZnO-Ms. and Au-NPS). After 24 h, the solution was centrifuged and dispersed in deionized water. The ZnO-MS were ultrasonically dispersed in ethanol for 10 min, and a drop of the solution was deposited on the exposed surface of a corning glass substrate, in the gap (about 500 μm) of a silver electrode. The above procedure was performed five times to achieve an electrical conducting path between the silver electrodes. For fabrication of the Au-NPs decorated ZnO-MS, five drops (on each case) of ZnO-MS and Au-NPs were alternately deposited on the substrate surface (Fig. 1a).

Electrical resistance values were similar on both pure ZnO-MS and Au-NPs decorated ZnO-MS, which discards out percolation originated by adjacent Au-NPs.

The gas response of the ether sensor was defined as follows:

$$Response\ (R) = \frac{R_g - R_a}{R_a}(100\%)$$

where R_a is the sensor resistance in presence of ambient dry air and R_g the sensor resistance in the presence of a mixture of wet air/

Table 1
Table of reagents used for synthesis of ZnO-MS and Au-NPs.

Reagent	Chemical formula	Purity (%)	Company
Zinc nitrate hexahydrate	$Zn\ (NO_3)2{\cdot}6H_2O$	98	Sigma-Aldrich
Hydrazine hydrate	H_6N_2O	Reagent grade	Sigma-Aldrich
Tetrachloroauric(III) acid	$HAuCl_4.XH_2O$	Assay 99.999	Sigma-Aldrich
Camellia sinensis extract		Conventional green tea bag	Lagg's

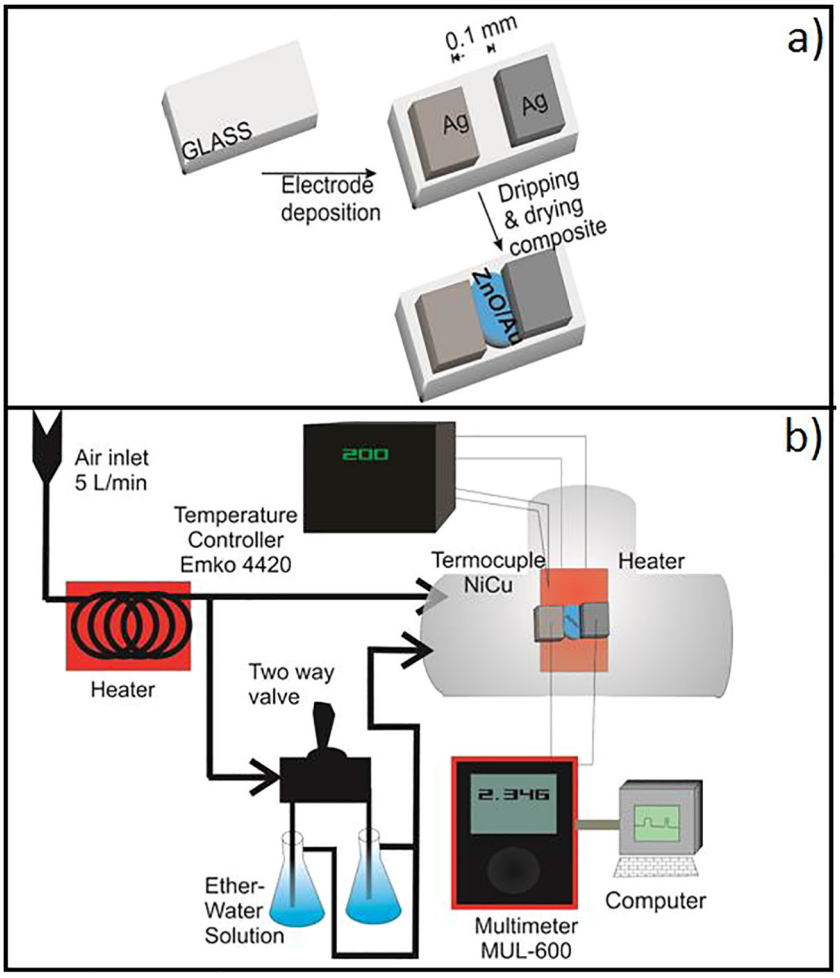

Fig. 1. a) Schematic illustration on the preparation of the Au-NPS decorated ZnO-MS, b) schematic diagram of the experimental arrangement for analysis of ether gas-sensing characteristics.

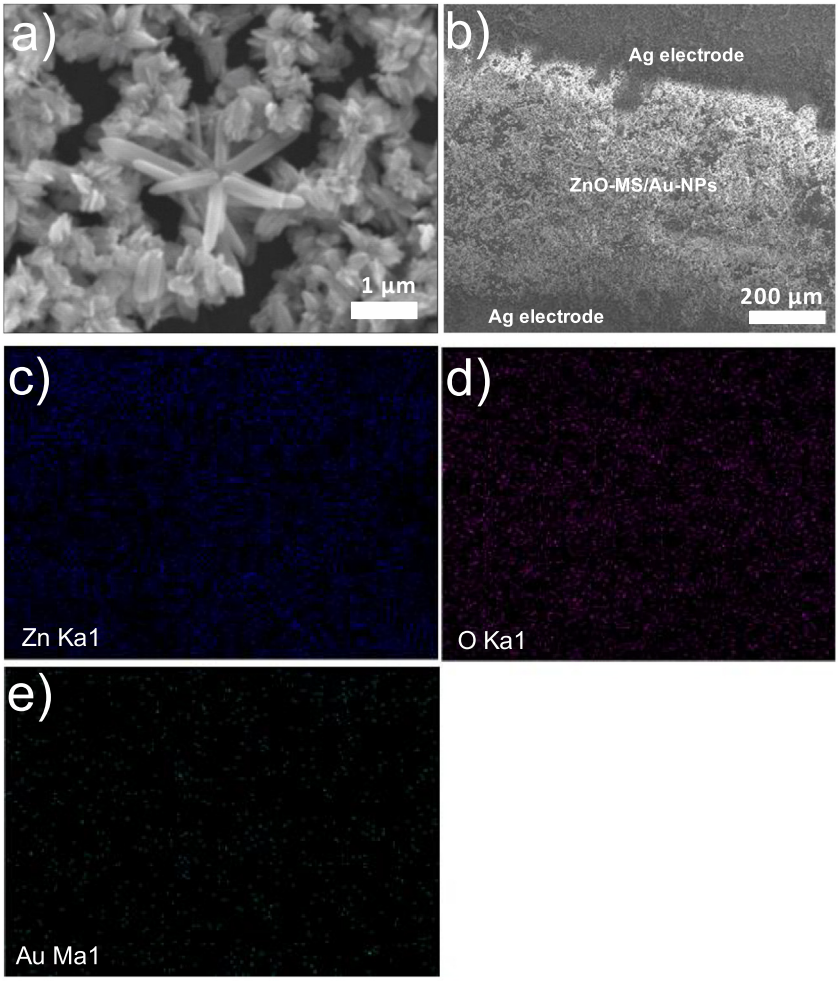

Fig. 2. SEM images and elemental EDX mapping of the Au-NPs decorated ZnO-MS: a) pure ZnO-MS; b) central zone where the Au-NPs decorated ZnO-MS was deposited, c) elemental mapping of Zn, d) elemental mapping of O, e) elemental mapping of Au, and f) elemental mapping of Au-NPs decorated ZnO-MS.

diethyl ether gas. The sensors fabricated with ZnO-MS and Au-NPs decorated ZnO-MS were tested for ether gas by using the set-up shown in Fig. 1b. The effective area for gas sensing was 5 mm^2 and the gas flow rate was 100 standard cubic centimeters per minute at atmospheric pressure. The thickness of the Au-NPs decorated ZnO-MS layer was 1 μm. The experimental procedure is described as follows: once the electrical resistance of the sensor was stabilized after fifteen minutes of heating the Au-NPs decorated ZnO-MS sensor at the working temperature, a mixture of ether/water was bubbled to the sensing chamber. According to the Henry's law, the partition constant of ether for air/water was determined to be 0.057 [26]. This value obtained by Lamarche and Droste in 1989 was used to estimate the concentrations of ether in the sensing chamber, which were 40, 200 and 400 mg ether/L of wet air for each case.

X-ray Diffraction (XRD) patterns were measured with a Bruker D8 Discover diffractometer using Cu Kα radiation (1.5418 Å). Transmission Electron Microscopy (TEM) and selected area electron diffraction (SAED) were carried out using a JEOL 2010 microscope operating at 200 kV accelerating voltage.

Results and discussion

Morphological and structural characterization

The general morphology of the pure ZnO-MS deposited on glass substrate is observed in Fig. 2a. As can be seen, the ZnO-MS are composed by aggregated rod-like particles, whose sizes are found in the nanometer scale. Fig. 2b exhibits the gap zone between the silver electrodes, where Au-NPs decoration of ZnO-MS was performed. Elemental EDX mapping revealed that Zn and O (Fig. 2c and d) were distributed homogenously throughout the deposition

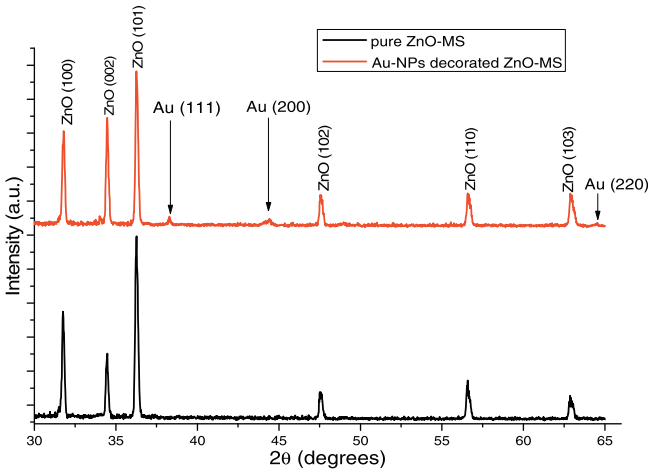

Fig. 3. XRD patterns of pure ZnO-MS and Au-NPs decorated ZnO-MS, which were active materials for fabrication of ether-gas sensors.

zone. Also, the Au atoms are randomly distributed on the surface of the gas sensor (ZnO-MS zone).

XRD characterization was performed to samples composed by pure ZnO-MS and Au-NPs decorated ZnO-MS (Fig. 3). Several peaks of the hexagonal ZnO lattice (JCPDS Card-File N_o. 36-1451) are observed in XRD patterns corresponding to both samples in 2Θ values at 31.80 (100), 34.49° (002), 36.22° (101), 47.56° (102), 56.60° (110), and 62.94° (103). In addition, three weak peaks of face-centered cubic Au lattice (JCPDS Card-File N_o. 04-0784) are observed for the Au-NPs decorated ZnO-Ms. sample in 2Θ values at 38.25° (111), 44.41° (200), and 64.44° (220). These results confirm formation of Au-NPs on the surface of the ZnO-MS.

Fig. 4a shows typical TEM micrographs of Au-NPs synthesized using *Camellia sinensis* aqueous extract. As seen in this figure, the micrograph shows different morphologies of anisotropic Au-NPs: triangular plates, decahedral, icosahedral, among others. The SAED pattern (Fig. 4b) revealed that the diffraction rings from inner to outer, with d-spacings of 0.2378 (A), 0.2201 (B), 0.141 (C), and 0.1297 (D), could be indexed as (111), (200),(220), and (311) reflections respectively, corresponding to face-centered cubic of Au. The diffraction rings also suggested the Au-NPs were polycrystalline. Fig. 4c shows TEM micrograph of ZnO-MS decorated with Au-NPs, which can be identified by superior contrast. Fig. 4e and f correspond to STEM-BF and STEM-ADF image of the ZnO-MS decorated with Au-NPS respectively. Au-NPs are located and well dispersed around the ZnO-MS in decorated-like array. Fig. 4d shows the SAED pattern measured from the ZnO-MS decorated with Au-Nps. This pattern revealed the presence of two phases. The d-spacings of 0.2332 (2), 0.1428 (4) and 0.1228 (5), could be indexed as (111), (220) and (311) reflections respectively, corresponding to FCC structure of Au. The numbers 1, 3, and 6 can be associated to (110), (104) and (102) reflections respectively, of the hexagonal ZnO structure (Table 2).

Gas sensing performance of ZnO and Au-NPs decorated ZnO-MS gas sensors

The gas sensing performance of pure ZnO-MS and the Au-NPs decorated ZnO-MS was monitored at working temperatures in the range of 150–250 °C. Upon exposure to different

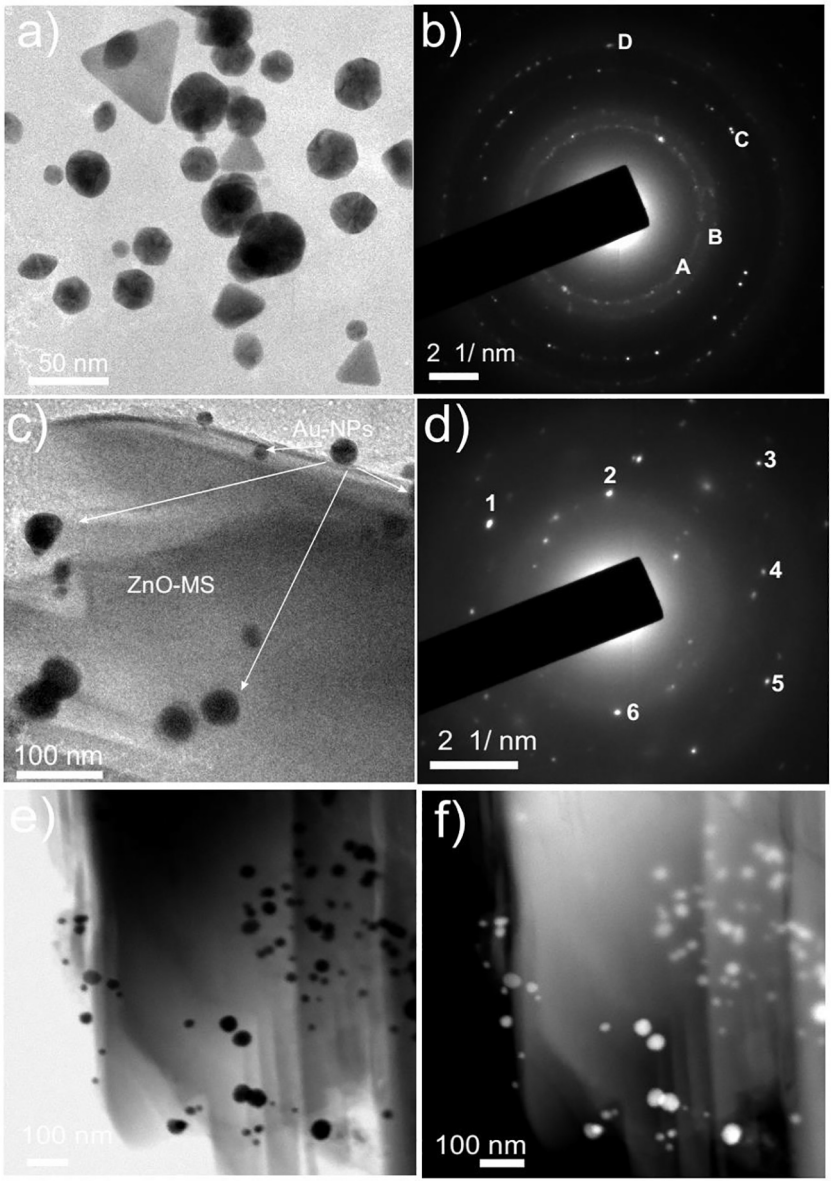

Fig. 4. Representative TEM micrograph and SAED pattern of Au-NPS (a) and (b), respectively. Au-NPs decorated ZnO-MS is shown in (c) TEM micrograph, (d) SAED pattern, (e) STEM-BF, and (f) STEM-ADF mode.

Table 2
Indexed interplanar distances measured from the Au-NPs decorated ZnO-MS.

	(hkl)	Interplanar values (nm)		Structure
		Theoretical	Experimental	
1	110	0.1624	0.1612	ZnO
2	111	0.2335	0.2332	Au
3	104	0.1181	0.1176	ZnO
4	220	0.1442	0.1428	Au
5	311	0.1230	0.1228	Au
6	102	0.1911	0.1899	ZnO

concentrations (40, 200, or 400 mg ether/L of wet air), sensors fabricated with pure ZnO-MS do not show any response to ether gas at temperature range of 150–200 °C. Only a weak sensitivity of about 25% was observed when the sensor was heated at 250 °C and exposed to a gas concentration of 400 mg ether/L of wet air (Fig. 5a). Although gas response from ZnO-based gas sensors depends upon the kind of gas to detect, it is known that the gas response is improved with the increase in the working temperature [27]. Fig. 5b shows the response curves from two replicative injections of ether (concentration of 400 mg ether/L of wet air) to the sensor fabricated with Au-NPs decorated ZnO-MS, heated at 250 °C. In contrast with pure ZnO-MS, sensor fabricated with Au-NPs decorated ZnO-MS showed better sensing characteristics in the selected temperature range. The response in both selected temperature range and ether gas concentrations for gas sensors fabricated with Au-NPs decorated ZnO-MS is shown in Fig. 5c. As can be seen, gas response is improved with increase in both working temperature and ether gas concentration. In fact, sensors fabricated with Au-NPs decorated ZnO-MS heated at 250 °C reached a gas response higher than that of ether gas sensor fabricated with pure ZnO-MS, independently of the ether gas concentration. The highest gas response was observed with the use of a gas concentration of 400 mg ether/L of wet air. As can be seen, at the highest both selected temperature and ether gas concentration, ether response increased from 25 to about 100% when Au-NPs are deposited on the surface of the ZnO-MS (Fig. 5d).

Gas sensing mechanism

The response of ZnO-based sensors is described and monitored as the change of electrical resistance. When ZnO is exposed to air, oxygen species are firstly adsorbed on its surface and then collect electrons from conduction band of ZnO to form oxygen ions [28]. Thus, an electron depletion layer (EDL) is formed near the surface of ZnO [29]. When reductive gas molecules from volatile organic compounds such as ethanol and acetone react with adsorbed

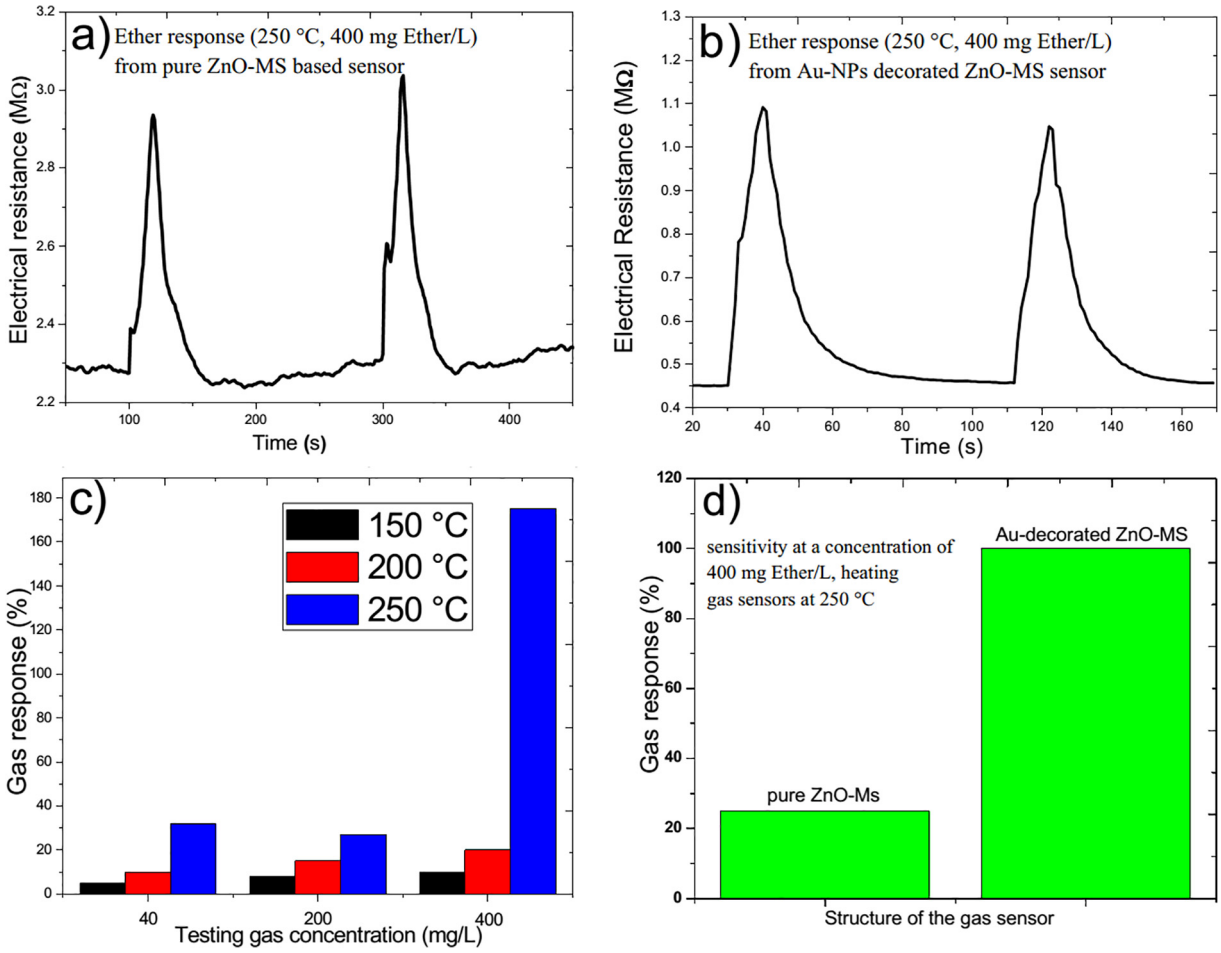

Fig. 5. Ether gas performance of Au-NPs decorated ZnO-MS-based sensor: a) response to pure ZnO-MS based sensor with the use of a temperature of 250 °C and a gas concentration of 400 mg ether/L of wet air, b) typical response curve to ether (working temperature 250 °C and gas concentration of 400 mg ether/L of wet air) for the Au-NPs decorated ZnO-MS-based sensor, obtained from two replicative ether gas injections, c) response of Au-NPs decorated ZnO-MS-based sensor to several working temperatures and different testing gas concentrations, d) gas response from both ZnO-MS and Au-NPs decorated ZnO-MS based sensors to 400 mg ether/L of wet air, heating the gas sensor at 250 °C.

oxygen ions, electrons are released and then injected to EDL, making it thinner [17]. Thus, electrical resistance of the ZnO-based gas sensor decreases. Some oxidative gases such as NO_2 and O_2 can also be detected using ZnO as active material [30,31]. When oxidative atoms are adsorbed on the surface of ZnO, they take away electrons from the surface of ZnO. Thus, the EDL becomes thicker and the electrical resistance increases [32]. In our experiment, when a pulse of ether is injected into the sensing chamber, ethyl peroxide (EPE) is formed by oxidation of ethyl ether at the working temperature [16]. Since EPE possess high oxidizability, it was expected that pure ZnO-MS-based sensor showed an appreciable change in electrical resistance when it was exposed to ether gas. However, as discussed above, only the sensor fabricated with pure ZnO-MS heated at 250 °C and exposed to a gas concentration of 400 mg/L showed a weak response of about 25%. Compared to the pure ZnO-MS, ether gas response was increased after deposition of Au-NPs to the ZnO-MS surface. This enhancement in the gas response can be explained by the mechanism known as spillover effect, which is a process where a catalytic dissociation of molecular oxygen occurs [21]. The Au-NPs catalytically activate dissociation of molecular oxygen into oxygen atoms on the surface of the ZnO-MS. As a result, concentration of oxygen atoms capable of trap electrons from conduction band of ZnO to form oxygen ions increases. As a result, EDL in ZnO becomes thicker due to the decreasing of electron concentration in ZnO, resulting in an increase of the electrical resistance.

Conclusions

In summary, ether gas sensing has been performed with the use of a sensor fabricated with Au-NPs decorated ZnO-MS in the temperature range of 150–250 °C. It was observed that increase in the working temperature improved the sensor response. For example, only the sensor fabricated with pure ZnO-MS and heated at the highest studied temperature (250 °C) exhibited an ether gas response. Similar behavior was observed for sensors fabricated with Au-NPs decorated ZnO-MS. In fact, when such sensors were exposed to a concentration of 400 mg ether/L of wet air, the gas response improved remarkably when the working temperature increased from 200 to 250 °C. In addition, at such working temperature and ether gas concentration, sensor composed by Au-NPs deposited on the surface of ZnO-MS showed a four times sensitivity higher than its counterpart fabricated with only pure ZnO-MS. Although efficient gas sensing for most ZnO-based gas sensors is usually observed for working temperatures higher than 300 °C, it was shown here that high response to ether gas can be obtained at 250 °C by deposition of Au-NPs to the surface of ZnO-MS. The enhancement on the ether sensing was associated to dissociation of molecular oxygen, which could by favored by the catalytic activity of the Au-NPs. The enhancement on the ether gas sensing was associated to dissociation of molecular oxygen, which could by favored by the catalytic activity of the Au-NPs.

Acknowledgments

The authors thank to Universidad Autónoma del Estado de México for financial support, through project number 1025/2014RIFC; to CCIQS for TEM measurements through project number EV-2015-1, and also to CONACYT for postdoctoral scholarship to Dr. Roberto López.

References

[1] Polat S. Fuel Process Technol 2016;143:140.
[2] Kim H, Hong J, Park Y, Kim J, Hwang I, Kang K. Adv Funct Mater 2015;25:534.
[3] Wikandari R, Nguyen H, Millati R, Niklasson C, Taherzadeh M. BioMed Res Int 2015;2015. http://dx.doi.org/10.1155/2015/494182. Article ID 494182, 6 pages.
[4] Baselt R. Disposition of Toxic Drugs and Chemical Drugs in Man. 10th ed. Seal Beach, CA: Biomedical Publications; 2014.
[5] MSDS number E2340, effective date: 10/15/97.
[6] Afonso C. Comprehensive Organic Chemistry Experiments for the Laboratory Classroom. United Kingdom: Royal Society of Chemistry; 2017.
[7] Zhang L, He N, Shi W, Lu C. Anal Bioanal Chem 2016;408:8787.
[8] Hu H, Li Q, Zhang L, Zeng B, Deng D, Lv Y. Anal Chem 2016;88:8137.
[9] Wang Q, Li B, Wang Y, Shou Z, Shi G. Luminescence 2014. http://dx.doi.org/10.1002/bio.2731.
[10] Davar F, Majedi A, Mirzael A. J Am Ceram Soc 2015;98:1739.
[11] Gómez C, Ballesteros JC, Torres L, Juárez I, Díaz LA, Zarazua M, Whon S. J Photochem Photobiol A 2015;298:49.
[12] Pauporté T, Lupan O, Zhang J, Tugsuz T, Ciofini LL, Labat F, Viana B. ACS Appl Mater Interfaces 2015;7:11871.
[13] Anku W, Oppong S, Shukla S, Govender P. Bull Mater Sci 2016;39:1745.
[14] Catto A, da Silva L, Ribeiro C, Bernardini S, Aguir K, Longo E, Mastelaro V. RSC Adv 2015;5:19528.
[15] Wen Z, Zhu L, Zhang Z, Ye Z. Sens Actuators B 2015;208:112.
[16] Kumar N, Srivastava A, Patel H, Gupta B, Varma G. Eur J Inorg Chem 2015;2015:1912.
[17] Cardoza M, Romo Jose, Rios Luis, García R, Zepeda T, Contreras O. Sensors 2015;15:30539.
[18] Feng Z. Zinc oxide and related materials. CRC Press; 2013. Vol. 1.
[19] Chen W, Gao T, Li Q, Gan H. Mater Technol 2015;30:96.
[20] Wang C, Yin L, Zhang L, Xiang D, Gao R. Sensors 2010;10:2088.
[21] Nakate U, Bulakhe R, Lokhande C, Kale S. Appl Surf Sci 2016;371:224.
[22] González J, Olvera M, Maldonado A, Reyes A, Meléndez M. Rev Mex Fis 2006;52:6.
[23] Majhi S, Rai P, Yu Y. ACS Appl Mater Interfaces 2015;7:9462.
[24] Kumar R, Al Dossary O, Kumar G, Umar A. Nano Micro Lett 2015;7:97.
[25] Gu F, Chen H, Han D, Wang Z. RSC Adv 2016;6:29727.
[26] Sander R. Atmos Chem Phys 2015;15:4399.
[27] Wang X, Sun F, Duan Y, Yin Z, Luo W, Huang Y, Chen J. J Mater Chem C 2015;3:11397.
[28] Kim J, Yong K. J Phys Chem C 2011;115:7218.
[29] Yoo R, Cho S, Song M, Lee W. Sens Actuators B 2015;221:217.
[30] Patil V, Vanalakar S, Patil P, Kim J. Sens Actuators B 2017;239:1185.
[31] Yadav K, Gahlaut S, Mehta B, Singh J. Appl Phys Lett 2016;108:071602.
[32] Kwon Y, Kang S, Mirzaei A, Choi M, Bang J, Kim S, Kim H. Sens Actuators B 2017. http://dx.doi.org/10.1016/j.snb.2017.04.053.